CEE-M
CENTER FOR ENVIRONMENTAL ECONOMICS - MONTPELLIER

Crop Prices and Deforestation in the Tropics

Nicolas Berman
Mathieu Couttenier
Antoine Leblois
&
Raphaël Soubeyran

CEE-M Working Paper 2021-14

Crop Prices and Deforestation in the Tropics

N. Berman[1], M. Couttenier[2], A. Leblois[3], and R. Soubeyran[3]

[1]*AMSE & CEPR*
[2]*ENS de Lyon & CEPR*
[3]CEE-M, Univ. Montpellier, CNRS, INRAE, Institut Agro, Montpellier, France

September 21, 2021

Abstract

Global food demand is rising, pushed by growing world population and dietary changes in developing countries. This encourages farmers to increase crop production which, in turn, increases worldwide demand for agricultural land and the pressure on tropical forests. With a possible doubling of world food demand by 2050, this pressure is not likely to decrease in the next decades. While the impact of food demand on deforestation has been pushed forward in the medias, rigorous evidence using large-N data estimating the causal impact of crop price variations on deforestation remains scarce. Here, we quantify this impact over the twenty first century using high resolution annual forest loss data across the tropics, combined with information about crop-specific agricultural suitability and annual international commodity prices. We find a sizeable impact of price variations on deforestation: crop price variations are estimated to have contributed to 35% of the total predicted deforestation in the tropics over the period 2001-2018. We also highlight that the degree of openness to international trade and level of economic development are first-order local characteristics to explain the magnitude of the impact of crop prices on deforestation.

1 Introduction

Tropical deforestation is one of the main causes of recent global environmental changes. Recent assessments revealed that food systems are responsible for a third of global anthropogenic GHG emissions [1] and that 17% of tropical moist forests have disappeared since 1990, with a remaining area of about one billion hectares in 2019, from which 10% are degraded [2]. Deforestation threatens crucial ecosystem services, such as biodiversity richness, climate regulation, carbon storage, water supplies, and leads to more infectious diseases [3, 4, 5, 6, 7, 8]. Market forces are among the most prominent determinants of tropical deforestation [9, 10], as they largely drive agricultural expansion [11, 12]. Forecasts point to a sharp increase in food demand over the next decades, with a possible doubling between 2017 and 2050 [13], which would drag crop prices in its wake. This will likely lead to a strong increase in land demand as private actors relate the amount of deforested area to the difference between the private value of forested and agricultural land [14].

In this paper, we estimate the effect of crop price variations to deforestation in the tropics. We combine different datasets at the spatial resolution of 0.5 degree latitude and longitude grid cells (approximately 55 $\times$ 55 kilometers at the equator) covering the tropics from 2001 to 2018. First, we make use of fine-grained estimates of yearly deforestation of 1 arc-second pixels (approximately 30 meters $\times$ 30 meters at the equator) [15]. For each cell, we compute the total number of pixels that are deforested during a year. Second, we gather cell-specific information on the agronomic suitability of 15 crops to proxy the potential crop specialization at the cell-level (Global Agro-Ecological Zones, [16]). We combine these data with the international prices of crops traded on international markets to construct a cell-specific, time-varying crop price index. This index is computed as the sum of the international prices of each crop in a given year, weighted by the relative agronomic suitability of each crop in the cell (see Methods in Section 4.1 and Supplementary Information (SI, hereafter) Section 9.1 and 9.2). Our final sample includes around fourteen thousands 0.5 $\times$ 0.5 degree cells over the period 2001-2018.

Our identification strategy uses within-cell variations in the crop price index and deforestation over time. We control for a large array of unobserved factors, namely all time-invariant cell characteristics and national time-varying shocks, that may correlate with both deforestation and world crop prices. We find that changes in crop prices significantly affect deforestation in the tropics. The effect is sizeable: the variations of our price index contribute to 35% of the total predicted deforestation over the period. We find that the effect of price variations significantly varies within countries depending on crop suitability and initial forest cover, as well as on the degree of exposure to international trade (proxied by distance to seaports), on the level of economic development (nightlight luminosity) and, to a lesser extent, state capacity (distance to the capital).

The presumption that international crop prices, boosted by global demand, contribute to tropical deforestation is not new. However, the empirical evidence to date continues to be largely based on cross-national comparisons [17, 18, 19, 20, 21, 22], focusing on a single country [23, 24, 25, 26], region [18], and with a limited number of commodities [27]. The usual approaches in global studies encompasses spatial attribution (based on crop-specific production maps [27] or spatial patterns recognition [10, 28]) and input-output [29, 30, 31] or trade and land-balance modelling [12, 32, 33]. These contributions typically use supply side models at the national level and downscale national trade or production data at the local-level. Our approach has several advantages: it is less data-demanding[1]; it is agnostic in terms of scale of agricultural production contrary to contributions based on spatial attribution or classifications methods [10, 28] that oppose large scale commodity driven deforestation to shifting agriculture[2]; it uses a sample based on forested areas at the beginning of the study period, rather than deforested areas at the end of the period, which facilitates causal interpretation; and it does not suffer from leakage effects since it is not limited to a single crop or geography [35].

Our study differs from this literature on other dimensions. First, we precisely estimate both the effect and the contribution of international crop prices variations to tropical deforestation over two decades, at a fine-grained level, yet at a global scale. Second, our approach combines exogenous local crops suitability – rather than production – with international crop prices, and controls for a large range of

[1]National data have well-known limitations. They are subject to omission bias stemming from undeclared activities such as home-based and locally-consumed agricultural production. A large share of smallholder production is consumed locally and not traded on international markets, such as oil in Sub-Saharan Africa [34]. Trade flow analyses and trade accounting methods are also limited by their lack of spatial explicitness, leading to imprecise links between consumption patterns and socio-environmental impacts in production regions [31]

[2]Because they rely on the recognition of spatial patterns these methods cannot be used to link production of – or demand for – commodities to small scale deforestation that may however also be, directly or indirectly, related to demand on international markets.

possible confounding factors not accounted for in previous studies. Finally, we highlight a number of policy-relevant local factors affecting how fluctuations in crop prices trigger deforestation.

2 Results

Crop prices and deforestation in the tropics. Figure 1 displays the main results estimated with an Ordinary Least Square (OLS) estimator[3]: the cell-specific crop price index is positively and significantly correlated to deforestation (the estimated coefficient is equal to 1.24 and the standard error to 0.08). The effect is sizeable: a 10% increase in the price index leads to a 12.4% [$\pm 1.6pp$] increase in deforestation (Figure 1, Model 1). As the potential for deforestation mechanically depends on the proportion of forest cover at the beginning of the period (SI Figure 7 maps the forest cover in 2000), we allow the effect of crop prices to vary across deciles of cell-specific forest cover in 2000 (Figure 1, Model 2). We find that the effect of crop prices increases with initial cover. For the first two deciles, the point estimate is not significantly different from 0; the coefficient then nearly triples between the third and the last decile. These results are robust to various sensitivity checks (SI Section 10.2): i) using an alternative threshold for the canopy cover at the beginning of the period; ii) excluding potentially influential observations (outliers); iii) estimating the model through a Poisson Pseudo-Maximum Likelihood (PPML) estimator; iv) allowing the standard errors for both cross-sectional spatial correlation and location-specific serial correlation [36] and v) focusing on countries which market share in agricultural commodities is low at the world level. This last exercise is particularly relevant: despite the fine-grained level of our analysis, and using potential rather than actual agricultural production, we cannot fully rule out that both deforestation and international commodity prices are simultaneously caused by supply-side shocks in large producing countries. Our results is largely unchanged when focusing only on small producers, which comforts our demand-side interpretation of the results.

Figure 1: Baseline effects of crop prices on deforestation

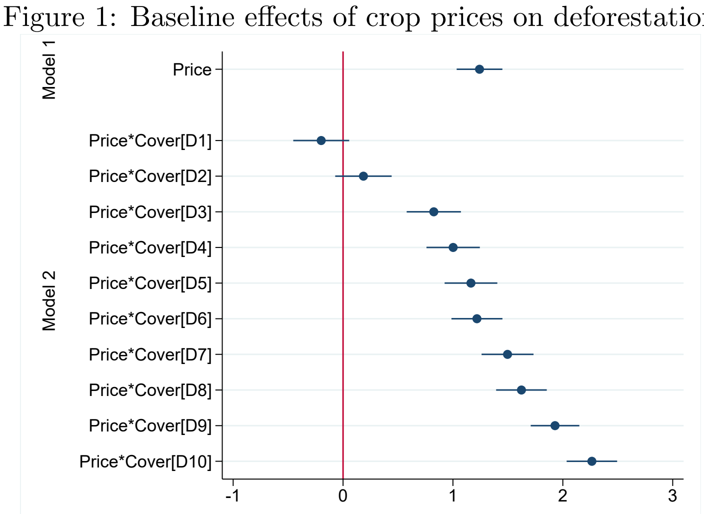

Note: Model 1 is the baseline estimate of the effect of the crop price index on deforestation, while Model 2 allows the effect of crops on deforestation to differ across deciles of forest cover at the beginning of the period (2000). See Section 4 and SI Section 10.1 for more details.

From 2001 to 2018, our crop price index has increased by more than 40% on average and the price of major crops such as maize, rice, oil-palm, soybean has increased by 45% to 85%. To get a sense of the role of this historical rise in crop prices, we use our estimates of Figure 1, Model 2 to estimate the total contribution of crop price variations to the observed predicted deforestation over this period. We find that the historical rise in crop prices contributed to 35% of predicted forest loss. Figure 2 reports spatial heterogeneity in the contributions across cells over the 2001-2018 period. Two features explain this pattern: heterogeneous crop suitability and hence variations of world prices (SI Figure 6), and the initial forest cover of the cell (SI Figure 7). A visual inspection reveals that the contribution of crop price variations has been the strongest in the three main tropical moist forest biomes: the Amazon, South-East Asia and, to a smaller extent West and Central Africa. Interestingly, and contrary to previous evidence, we find that all tropical forests are subject to land pressure stemming from shocks in the

[3]Full estimations results available in SI Table 2.

Figure 2: Contribution of crop prices variations to deforestation, 2001-2018

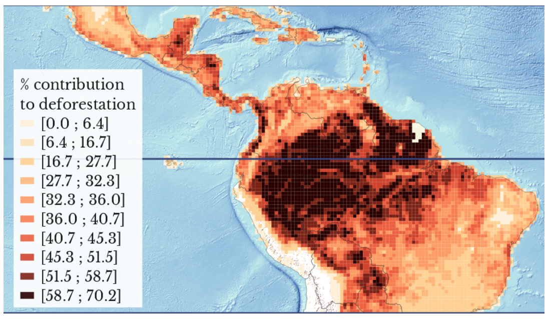

(a) Americas

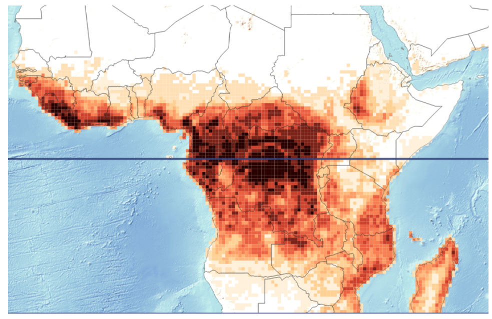

(b) Africa

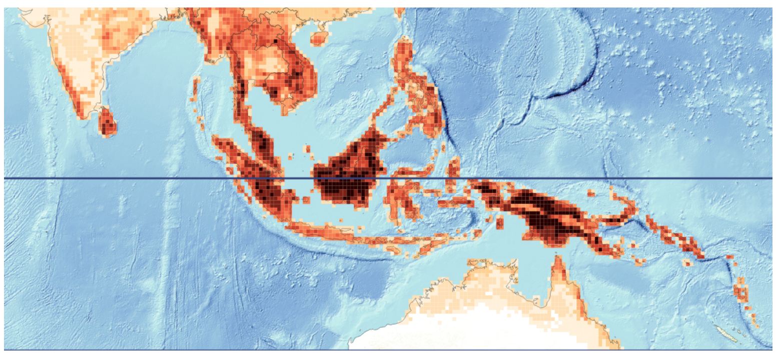

(c) Asia and Oceania

Note: Contribution of crop price variations to deforestation. Quantification based on the estimation results of Model 2 (see Methods in Section 4.1). We first compute the predicted level of deforestation using observed prices, our benchmark). Then we compute a counterfactual level of deforestation assuming fixing prices at their 2001 level. Finally, we sum these predictions by cell over the period, and compute for each cell the contribution of prices as the difference between the benchmark and the counterfactual predictions, divided by the counterfactual.

prices of internationally traded commodities. For instance, our results tend to validate recent evidence indicating that, despite cropland expansion in sub-Saharan Africa being still dominated by production for domestic markets, there is a growing influence of global markets on change in land use in the region [18].

Trade costs and other local characteristics. Our main results suggest that areas witnessing stronger increases in the prices of locally suitable crops experience faster deforestation. It is likely, however, that other local characteristics may dampen or exacerbate the contribution of crop price variations to deforestation. First, as suggested by the literature [14, 37, 38], we expect openness to international trade to exacerbate the role played by crop prices. Second, local institutional quality and the capacity of states to enforce property rights may also affect the sensitivity of deforestation to crop prices [11]. Indeed, under open access regimes for instance, rational farmers should theoretically rush to exploit land and cut forest more quickly [37, 39]. The impact of the formalisation of land rights and land tenure on forest loss has been demonstrated in the case of a land registration program in Benin [40], in the case of a land titling program in the Brazilian Amazon [41] and the role of customary tenure systems on deforestation has also been exposed in the case of Cameroon [42].

We consider these potential mitigation factors by interacting cell-specific characteristics with our price index in our baseline models. To measure the cell-specific exposure to international trade, we use information on the distance of the cell's centroid to the closest major seaport as a proxy of transportation costs [14]. To measure institutional quality at the local-level, we use the distance between the cell's centroid and the capital city of the country. Rule of law, property rights protection and more generally institutional quality are expected to be weaker in places located far from the capital [43]. Finally, we consider a measure of nighttime luminosity to proxy local economic development [44, 45], taken at the beginning of the sample period to avoid reverse causality concerns. State capacity and institutional quality are also expected to be stronger in wealthier locations. All cell-specific variables have been standardized to make coefficients comparable.

Figure 3: Cell-level characteristics

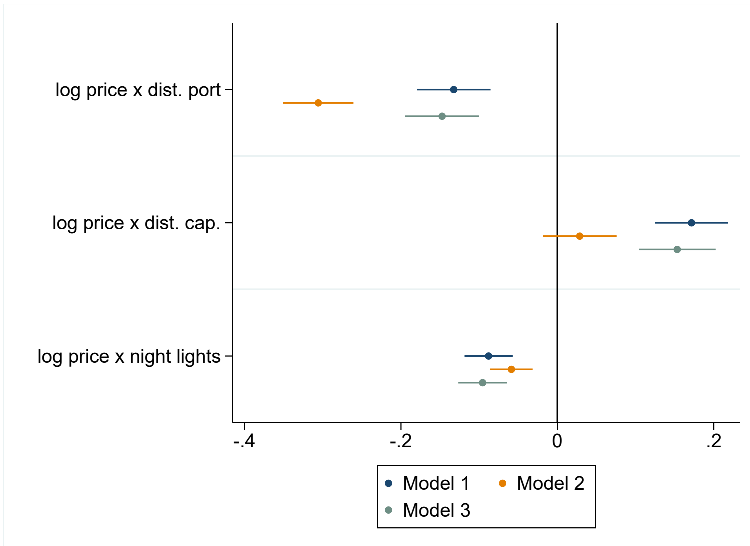

Note: The figure displays the point estimates and confidence interval of the effect of the interaction between cell-specific characteristics and our prices index. Model 1 uses the baseline specification, augmented with interaction terms between the price index and (standardized) cell-characteristics variables (see SI Sections 4 and 10.1). Model 2 allows the effect of crop price on deforestation to vary across the deciles of the initial forest cover distribution. Model 3 controls for a full set of interaction terms between country dummies and the price index.

The standardized estimates of the interaction terms between cell-level characteristics and crop prices are plotted in Figure 3 (the full estimates are available in SI Table 3). Figure 3 considers three models: Models 1 and 2, as in Figure 1; and Model 3, which enables for heterogeneous effects of the price index between countries. In the latter, we purge the estimates of the interaction terms from their country-wide component (e.g., differences in country size), focusing solely on within-country variations in cells characteristics. First, we find that the positive effect of crop price variations on deforestation is significantly stronger in cells that are close to a seaport, suggesting that openness to international trade exacerbates the effect of crop prices variations on deforestation. Second, cells that are less economically developed display a stronger sensitivity to crop price variations. Finally, though the significance of the estimates fluctuates more, our results point to larger commodity-driven deforestation in cells that are more distant from the capital city – i.e. locations with weaker state capacity. On average across specifications, distance to port has the stronger effect. This supports the key role of access and exposure to international trade. The effect of trade costs and economic development are barely affected by our sensitivity checks; the effect of local state capacity is less robust (SI Section 10.2.2).

To illustrate these results, we focus on the Congo Basin, a major tropical moist forest biome spanning several countries. We first repeat the quantification exercise of Figure 2, restricting the sample to countries of the Congo Basin. The results are shown in Figure 4.a, which displays for each cell the contribution of crop price variations to predicted deforestation over the period, as well as the location of major seaports and of the capital cities of each country. Second, we repeat this quantification exercise but using the specification that includes interactions with cell characteristics (Model 2 of Figure 3). Figure 4.b plots the difference in percentage points between the two quantification exercises. Clearly, being close to a port has the strongest effect on commodity-driven deforestation. However, regions extremely distant from the capital city, though they are less exposed to international trade (e.g. the border between Cameroon and Central African Republic), also display significant effects. Having a visual inspection of the same exercise for the full set of regions in the tropics delivers the same striking spatial patterns (Figure 8 in SI Section 10.3)

3 Discussion

We find that changes in crop prices significantly affect deforestation in the tropics at the local-level; this confirms the key role of market forces [12]. We bring robust statistical evidence that the many farm commodities and products traded daily on international markets are contributing to a large share of global

Figure 4: Focus on the Congo Basin

(a) Baseline quantification (b) Additional contribution of cell-level characteristics

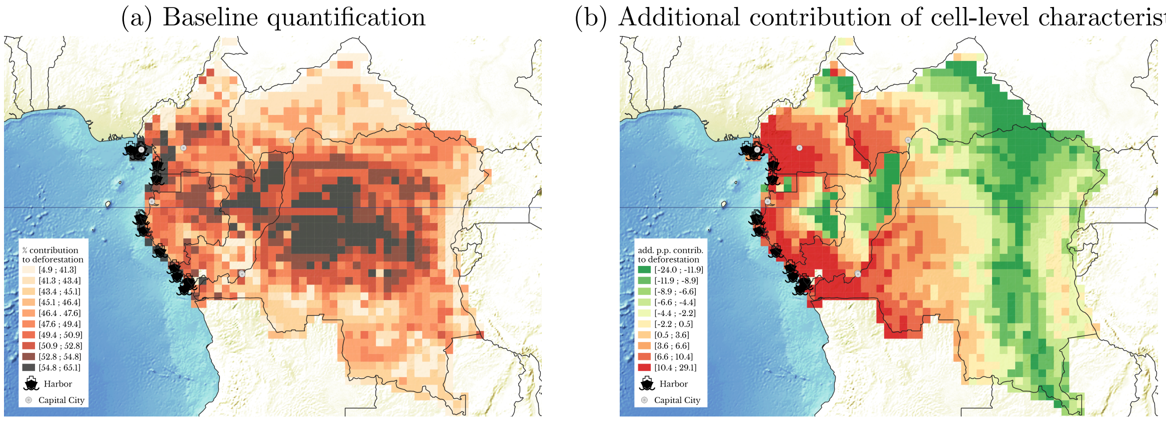

Note: Figure (a) shows the contribution of crop price variations to forest loss, sample restricted to the Congo Basin. Quantification based on the estimation results of Model 2 (see Methods in section 4). We first compute the predicted level of deforestation using observed prices, our benchmark. Then we compute a counterfactual level of deforestation assuming fixing prices at their 2001 level. Finally, we sum these predictions by cell over the period, and compute for each cell the contribution of prices as the difference between the benchmark and the counterfactual predictions, divided by the counterfactual. Figure (b) shows the difference in p.p. between Figure (a) and the sample quantification based on a specification where interaction terms between prices and cell characteristics are included.

deforestation. As the demand for these products increases, new arable land is required for commodity crops. In this context, the natural solution to tackle deforestation goes through the demand side: if consumers reduce their demand for agricultural products, crop prices will stabilize and deforestation will likely slow down. However, forecasts about the evolution of demand over the next decades suggest that a drop in demand is unlikely [13]. Policies targeting consumers' preferences and behavior should therefore be combined with measures aiming at directly slowing down deforestation. Such measures involve multiple actors – companies, NGOs and governments. Firms can implement strategies such as supply chain initiatives promoting larger transparency, or adopt unilateral or multilateral commitments. The complexity of the supply chains, the possibility of leakage, low and selective adoption, and the risk of marginalization of smallholders make the impact of these actions uncertain [46] – as illustrated, for instance, by the case of palm oil supply chains [47]. On the other hand, national and local governments, with the help of NGOs, can implement various policies to reduce deforestation. These policies include encouraging dietary changes, mandating transparency in supply chains, incentivizing companies to adopt effective anti-deforestation strategies, penalizing companies responsible for significant deforestation, or implementing programs to reduce the sensitivity of community incomes to international crop prices. The development of monitoring tools such as the Trase initiative (*Transparency for Sustainable Economies*)[4] and more generally the development of real-time information on areas at risk of deforestation, by improving monitoring by local and national actors, could facilitate the application of anti-deforestation policies.

4 Methods

4.1 Data

We consider a full set of grid cells of the tropics, i.e. the area between the Tropic of Cancer at 23°26' N and the Tropic of Capricorn at 23°26' S, divided in sub-national units of 0.5×0.5 degrees latitude and longitude. Our unit of observation in our dataset is a cell-year; that is, we estimate how variations in crop prices affect deforestation in a given cell during a given year, over the 2001-2018 period.

Deforestation. We use the tree cover loss data from Hansen *et al.* [15]. Thanks to Landsat data, they define a tree cover loss as a stand-replacement disturbance or the complete removal of tree cover canopy at the pixel scale. The original data contain an estimation of the annual tree cover loss for the period 2001-2018 (see SI Section 9.1), relative to the 2000 forest cover, for pixels at a spatial resolution of 1 arc-second (around 30 meters). In the baseline estimates, we consider a 1 arc-second pixel as being a

[4]The Transparency for Sustainable Economies initiative is an online platform aimed at improving the transparency, clarity and accessibility of information on the commodity supply chains that drive tropical deforestation.

forest when the forest cover in year 2000 is larger than 25%, as in global studies using the same data [48, 49, 50]. Alternatively, we use a 50% canopy threshold in our sensitivity analysis (see SI Section 10.2). For each of these thresholds, we count the number of pixels defined as deforested within each 0.5×0.5 degrees cell-year – this is our baseline measure of deforestation.

Crop Price Index. We rely on information on international crop prices and agronomic suitability to build our price index. Our index uses information for 15 crops, traded on international market places, for which both annual international price and suitability data are available: banana, barley, cocoa, coconut, coffee, cotton, maize, oil palm, rice, sorghum, soybean, sugar, tea, tobacco and wheat. International crop prices (base 100 in 2000) come from the World Bank Commodity Dataset [51]. The time-invariant agronomic suitability [16] comes from the Global Agro-Ecological Zones (GAEZ, FAO[5]). It is defined as the percentage of the maximum yield that can be attained in each grid cell. For each cell c and year t, we compute the international market price of crops based on the cell-specific relative suitability of each crop i, i.e. for each cell, the suitability of the crop divided by the sum of the suitability of all the crops:

$$\text{Price}_{c,t} = \sum_{i=1}^{15} \alpha_c^i \times P_t^i, \tag{1}$$

where α_c^i is the relative suitability of crop i in cell c and P_t^i is the average price of crop i during year t. Our first identification assumption is therefore that fluctuations in the prices of, say, rice, affects primarily areas suitable to grow rice. Our second identification assumption is that $\text{Price}_{c,t}$ is not affected by deforestation or by other time-varying determinants of deforestation. Suitability (α_c) being mostly related to natural soil characteristics, and not to actual crop production, it is arguably exogenous to changes in deforestation. We assume that prices (P_t^i) are also exogenous to cell-year deforestation and its drivers, given our level of spatial aggregation. However, because we cannot rule out the possibility that supply side shocks in large producing countries affect world prices, we also show that all our results are largely insensitive to the exclusion of large producers (SI Table 10).

Final Sample. Our final sample covers the period 2001-2018 and is composed of 13,999 cells, for which agronomic suitability data is available and forest cover in 2000 is strictly positive, i.e, at least 1 arc-second pixel as forest when the canopy threshold is larger than 25% of the cover. Our dataset is therefore a balanced panel of 251,982 observations. Summary statistics appear in SI Table 1.

Preliminary evidence. Over the 2001-2018 period, the SI Figure 5 shows the accumulated deforestation for each pixel and the SI Figure 6 displays the average price index variations. Interestingly, South America (the Amazon) and South-East Asia (Indonesia forests) display both the highest deforestation rates and the highest price index variations over the period.

4.2 Estimation

Estimated models. In the Model 1, we estimate the impact of the log of the crop price index ($\ln \text{Price}_{c,t}$) on the inverse hyperbolic sine transformation of the number of deforested pixels ($\text{Deforest}_{c,t}$)[6] in cell c during year t, controlling for cell and for country $\times$ year fixed effects (η_c and $\nu_{country,t}$, respectively):

$$\text{Deforest}_{c,t} = \beta \ln \text{Price}_{c,t} + \eta_c + \nu_{country,t} + \varepsilon_{c,t}, \tag{2}$$

where ε_{ct} is the error term. Standard errors are clustered by cell in the baseline, and in our sensitivity analysis we allow for spatially correlated errors within larger radius. The aim of the cell fixed effects is to control for any time-invariant cell characteristics which may correlate with both the average deforestation rates and crop prices (e.g. geography, topography, soil characteristics). The inclusion of country $\times$ year fixed effects ($\nu_{country,t}$) accounts for any time-variant country characteristics such as global trends in overall crop prices, nation-wide shocks or policy changes that may trigger or hamper deforestation. To study the role of local characteristics, with use specifications where (2) is augmented with interactions terms between $\ln \text{Price}_{c,t}$ and cell-specific proxies of trade openness, development or state capacity. Throughout the paper, as deforestation is bounded by the initial forest cover, we allow the effect of price ($\ln \text{Price}_{c,t}$) to vary across deciles of forest cover (Model 2); we also allow it to vary across countries (Model 3) when

[5]GAEZ, FAO data, available here: http://www.fao.org/nr/gaez/about-data-portal/en/

[6]This transformation is frequently used in applied econometric work, because it approximates the natural logarithm while allowing to keep zero-valued observations in the estimation [52, 53, 54].

looking at the effect of cell characteristics. We estimate the models trough an Ordinary Least Square (OLS) estimator in the baseline estimates and use a Poisson Pseudo Maximum Likelihood (PPML) estimator in our sensitivity exercises.

Sensitivity analysis. The sensitivity analysis of the estimates of Models 1 and 2, and their versions augmented with cell characteristics, are displayed in SI Section 10.1. For each estimation, we consider the following robustness:

- As our main dependent variable is a count of the number of deforested pixels, we estimate the model through a Poisson Pseudo-Maximum Likelihood (PPML) estimator.
- We consider an alternative canopy threshold that defines the tropical forest biome at 50% instead of 25%. This second definition of forest is more conservative and ensures that 30m pixels contain enough tree cover in 2000 to be considered as a forest biome.
- We assess the robustness of the main results to potential outliers, i.e. we check that our results are not driven by a small number of extreme observations. We exclude observations that are 1, 2 and 3 standard deviations away from the residual mean.
- Another concern is that our results could be driven by a small number of countries, especially those who might influence the world price of agricultural commodities. For each country and crop, we compute the average market share in world trade over our period of study, and drop from our estimations the countries belonging to the top 10%, 25% and 50% of our sample in terms of world market share.
- The fine-grained dimension of our analysis makes it likely that the error term exhibits both spatial and serial correlation. To address this, we check that our results are robust to a non-parametric standard errors estimation [36, 55], allowing for both cross-sectional location-specific serial correlation, as well as spatial correlation within a 500 or 1000km radius.

5 Data availability

The data that support the findings of this study is openly available at http://doi.org/10.5281/zenodo.4916785

6 Code availability

The code that support the findings of this study is openly available at http://doi.org/10.5281/zenodo.4916785

References

[1] Crippa, M. *et al.* Food systems are responsible for a third of global anthropogenic GHG emissions. *Nature Food* (2021).

[2] Vancutsem, C. *et al.* Long-term (1990-2019) monitoring of forest cover changes in the humid tropics. *Science Advances* **7**, eabe1603 (2021).

[3] Foley, J. A. *et al.* Global consequences of land use. *Science* **309**, 570–574 (2005).

[4] Turner, B. L., Lambin, E. F. & Reenberg, A. The emergence of land change science for global environmental change and sustainability. *Proceedings of the National Academy of Sciences* **104**, 20666–20671 (2007).

[5] Le Quéré, C. *et al.* Global carbon budget 2016. *Earth System Science Data* **8**, 605–649 (2016).

[6] Alkama, R. & Cescatti, A. Biophysical climate impacts of recent changes in global forest cover. *Science* **351**, 600–604 (2016).

[7] Song, X.-P. *et al.* Global land change from 1982 to 2016. *Nature* **560**, 639–643 (2018).

[8] Chaves, L. S. M. *et al.* Global consumption and international trade in deforestation-associated commodities could influence malaria risk. *Nature communications* **11**, 1–10 (2020).

[9] Geist, H. J. & Lambin, E. F. Proximate causes and underlying driving forces of tropical deforestation: Tropical forests are disappearing as the result of many pressures, both local and regional, acting in various combinations in different geographical locations. *BioScience* **52**, 143–150 (2002).

[10] Curtis, P. G., Slay, C. M., Harris, N. L., Tyukavina, A. & Hansen, M. C. Classifying drivers of global forest loss. *Science* **361**, 1108–1111 (2018).

[11] Angelsen, A. Agricultural expansion and deforestation: modelling the impact of population, market forces and property rights. *Journal of Development Economics* **58**, 185 – 218 (1999).

[12] Pendrill, F. *et al.* Agricultural and forestry trade drives large share of tropical deforestation emissions. *Global Environmental Change* **56**, 1–10 (2019).

[13] Fukase, E. & Martin, W. Economic growth, convergence, and world food demand and supply. *World Development* **132**, 104954 (2020).

[14] Souza-Rodrigues, E. Deforestation in the Amazon: A unified framework for estimation and policy analysis. *Review of Economic Studies* **86**, 2713–2744 (2019).

[15] Hansen, M. C. *et al.* High-resolution global maps of 21st-century forest cover change. *Science* **342**, 850–853 (2013).

[16] Fischer, G. *et al.* Global agro-ecological zones (GAEZ v3. 0)-model documentation (2012).

[17] Leblois, A., Damette, O. & Wolfersberger, J. What has driven deforestation in developing countries since the 2000s? evidence from new remote-sensing data. *World Development* **92**, 82–102 (2017).

[18] Ordway, E. M., Asner, G. P. & Lambin, E. F. Deforestation risk due to commodity crop expansion in sub-Saharan Africa. *Environmental Research Letters* **12**, 044015 (2017).

[19] Angelsen A, K. D. Rethinking the causes of deforestation: lessons from economic models. *World Bank Research Observer* **14**, 73–98 (1999).

[20] DeFries, R. S., Rudel, T., Uriarte, M. & Hansen, M. Deforestation driven by urban population growth and agricultural trade in the twenty-first century. *Nature Geoscience* **3**, 178–181 (2010).

[21] Hosonuma, N. *et al.* An assessment of deforestation and forest degradation drivers in developing countries. *Environmental Research Letters* **7**, 044009 (2012).

[22] Rudel, T. K. *et al.* Agricultural intensification and changes in cultivated areas, 1970–2005. *Proceedings of the National Academy of Sciences* **106**, 20675–20680 (2009).

[23] Hargrave, J. & Kis-Katos, K. Economic causes of deforestation in the brazilian amazon: a panel data analysis for the 2000s. *Environmental and Resource Economics* **54**, 471–494 (2013).

[24] Harding, T., Herzberg, J. & Kuralbayeva, K. Commodity prices and robust environmental regulation: Evidence from deforestation in brazil. *Journal of Environmental Economics and Management* **108**, 102452 (2021).

[25] Doggart, N. *et al.* Agriculture is the main driver of deforestation in Tanzania. *Environmental Research Letters* **15**, 034028 (2020).

[26] Faria, W. R. & Almeida, A. Relationship between openness to trade and deforestation: Empirical evidence from the Brazilian Amazon. *Ecological Economics* **121**, 85–97 (2016).

[27] Goldman, E. D., Weisse, M., Harris, N. & Schneider, M. Estimating the role of seven commodities in agriculture-linked deforestation: Oil palm, soy, cattle, wood fiber, cocoa, coffee, and rubber. *World Resources Institute Technical Note* 1–25 (2020).

[28] Austin, K. G., Schwantes, A., Gu, Y. & Kasibhatla, P. S. What causes deforestation in Indonesia? *Environmental Research Letters* **14**, 024007 (2019).

[29] Hoang, N. T. & Kanemoto, K. Mapping the deforestation footprint of nations reveals growing threat to tropical forests. *Nature Ecology & Evolution* 1–9 (2021).

[30] Green, J. M. *et al.* Linking global drivers of agricultural trade to on-the-ground impacts on biodiversity. *Proceedings of the National Academy of Sciences* **116**, 23202–23208 (2019).

[31] Godar, J., Persson, U. M., Tizado, E. J. & Meyfroidt, P. Towards more accurate and policy relevant footprint analyses: tracing fine-scale socio-environmental impacts of production to consumption. *Ecological Economics* **112**, 25–35 (2015).

[32] Pendrill, F., Persson, U. M., Godar, J. & Kastner, T. Deforestation displaced: trade in forest-risk commodities and the prospects for a global forest transition. *Environmental Research Letters* **14**, 055003 (2019).

[33] Henders, S., Persson, U. M. & Kastner, T. Trading forests: land-use change and carbon emissions embodied in production and exports of forest-risk commodities. *Environmental Research Letters* **10**, 125012 (2015).

[34] Ordway, E. M., Naylor, R. L., Nkongho, R. N. & Lambin, E. F. Oil palm expansion and deforestation in southwest Cameroon associated with proliferation of informal mills. *Nature communications* **10**, 1–11 (2019).

[35] Song, X.-P. *et al.* Massive soybean expansion in south america since 2000 and implications for conservation. *Nature Sustainability* (2021). URL `https://doi.org/10.1038/s41893-021-00729-z`.

[36] Conley, T. G. GMM estimation with cross-sectional dependence. *Journal of Econometrics* **92**, 1–45 (1999).

[37] Ferreira, S. Deforestation, property rights, and international trade. *Land Economics* **80**, 174–193 (2004).

[38] Abman, R. & Lundberg, C. Does free trade increase deforestation? the effects of regional trade agreements. *Journal of the Association of Environmental and Resource Economists* **7**, 35–72 (2020).

[39] Chichilnisky, G. North-south trade and the global environment. *American Economic Review* **84**, 851–874 (1994).

[40] Wren-Lewis, L., Becerra-Valbuena, L. & Houngbedji, K. Formalizing land rights can reduce forest loss: Experimental evidence from Benin. *Science Advances* **6**, eabb6914 (2020).

[41] Probst, B., BenYishay, A., Kontoleon, A. & dos Reis, T. N. Impacts of a large-scale titling initiative on deforestation in the Brazilian Amazon. *Nature Sustainability* **3**, 1019–1026 (2020).

[42] Ordway, E. M., Naylor, R. L., Nkongho, R. N. & Lambin, E. F. Oil palm expansion in Cameroon: Insights into sustainability opportunities and challenges in Africa. *Global Environmental Change* **47**, 190–200 (2017).

[43] Michalopoulos, S. & Papaioannou, E. National institutions and subnational development in Africa. *Quarterly Journal of Economics* **129**, 151–213 (2014).

[44] Henderson, J. V., Storeygard, A. & Weil, D. N. Measuring economic growth from outer space. *American Economic Review* **102**, 994–1028 (2012).

[45] Bruederle, A. & Hodler, R. Nighttime lights as a proxy for human development at the local level. *PloS one* **13**, e0202231 (2018).

[46] Lambin, E., Gibbs, H., Heilmayr, R. & et al. The role of supply-chain initiatives in reducing deforestation. *Nature Clim Change* **8**, 109–116 (2018).

[47] Lyons-White, J. & Knight, A. T. Palm oil supply chain complexity impedes implementation of corporate no-deforestation commitments. *Global Environmental Change* **50**, 303–313 (2018).

[48] Heino, M. *et al.* Forest loss in protected areas and intact forest landscapes: a global analysis. *PloS one* **10**, e0138918 (2015).

[49] Potapov, P., Hansen, M. C., Stehman, S. V., Loveland, T. R. & Pittman, K. Combining modis and landsat imagery to estimate and map boreal forest cover loss. *Remote sensing of environment* **112**, 3708–3719 (2008).

[50] Hansen, M. C., Stehman, S. V. & Potapov, P. V. Quantification of global gross forest cover loss. *Proceedings of the National Academy of Sciences* **107**, 8650–8655 (2010).

[51] World Bank Group. Commodity markets outlook, october 2020 (2020). Https://openknowledge.worldbank.org/handle/10986/34621 , License: CC BY 3.0 IGO.

[52] Burbidge, J. B., Magee, L. & Robb, A. L. Alternative transformations to handle extreme values of the dependent variable. *Journal of the American Statistical Association* **83**, 123–127 (1988).

[53] MacKinnon, J. G. & Magee, L. Transforming the dependent variable in regression models. *International Economic Review* **31**, 315–339 (1990).

[54] Pence, K. M. The role of wealth transformations: An application to estimating the effect of tax incentives on saving. *B.E. Journal of Economic Analysis & Policy* **5** (2006).

[55] Hsiang, S. M., Meng, K. C. & Cane, M. A. Civil conflicts are associated with the global climate. *Nature* **476**, 438–441 (2011).

7 Author contributions

All authors contributed equally to the study.

8 Competing interests

The authors declare no competing interests.

Supplementary Information (SI) – not for publication –

9 Data

9.1 Tree cover and deforestation

Information on tree cover for the year 2000 is available at a resolution of 1 arc-second (around 30m×30m). The tree cover is defined by Hansen *et al.* [15] as canopy closure for all vegetation taller than 5m in height. We consider two thresholds to consider a pixel as a forest: a canopy cover threshold of 25 and 50% of a pixel in year 2000. The main results define forest pixel as having at least 25% of forest cover, while robustness checks were run for a threshold of 50% (SI Section 10.2). Hansen *et al.* [15] estimates tree cover loss annually over the 2001-2018 period (version 1.6), defined as a stand-replacement disturbance, or a change from a forest to non-forest state. The data provides a year of tree cover loss for every pixel with more than 1% of forest cover (vegetation taller than 5m height) in 2000 that is estimated to endure a loss of more than 50% of the 2000 forest cover between 2001 and 2018. We consider that the whole pixel (30x30m) tree cover was reduced to zero when losses occur. Forest degradation, for example selective removals from within forested stands that do not lead to a non-forest state, was not included in the change characterisation. Moreover, the data does not allow to distinguish quality of the canopy and select every vegetation higher than 5m, potentially leading to consider secondary forest loss as deforestation.

9.2 Suitability

A crucial information to define our cell-specific price crop index is the crop-specific agronomic suitability of a cell. The FAO provides for the suitability for 45 crops at a resolution of 5 arc minute (FAO's global agroecological zones, GAEZ). These data are constructed from models that use location characteristics, such as climate information (rainfall and temperature, for instance) and soil characteristics. This information is then combined with crops' characteristics (in terms of growing requirements) to generate a global GIS raster of the suitability for each of the 45 crops. Constrained by the availability of international price data, our final sample encompasses 15 crops.

9.3 Other data

Throughout the manuscript we make use of different datasets. First, we use yearly information on night-time lights aiming to approximate local economic development.[7] Second, we compute the geodesic distances between each grid cell of 0.5×0.5 degree longitude and latitude and the closest port. We use location of ports around the World from *World Port Index* dataset[8] that provides GPS location of ports with a depth larger than 11 meters. Third, we compute the geodesic distance between each grid cells and the capital city of each country from PRIO-GRID.[9] Fourth, to compute the crop-specific country market share in world trade, we make use of the dataset on exports and imports from the FAO.[10]

9.4 Summary statistics

Table 1 displays the summary statistics of all variables used in the paper.

[7] Data from the DMSP-OLS, Nighttime Lights Time Series Version 4 (Average Visible, Stable Lights, & Cloud Free Coverages), as available in PRIO-GRID.

[8] Available at the following link: https://msi.nga.mil/Publications/WPI

[9] We use the distance to the capital city at the beginning of the period, as in a very small number of cases the capital city has changed during the period.

[10] Faostat data site: http://www.fao.org/faostat/en

Table 1: Summary statistics

Variable	Mean	Std. Dev.	Min.	Max.	N
Forest cover in 2000 (forest: > =25%)	1899521.45	1543807.74	1	4000000	251982
Forest cover in 2000 (forest: > =50%)	1523987.16	1528444.94	0	4000000	251982
Deforestation (pixel share, forest: > =25%)	0.006	0.028	0	1	251982
Deforestation (pixel share, forest: > =50%)	0.008	0.033	0	1	240750
Deforestation (pixel count, forest: > =25%)	9276.58	21691.43	0	749160	251982
Deforestation (pixel count, forest: > =50%)	7977.64	20306.19	0	746363	251982
Inverse hyperbolic sine transformation of Deforestation (pixel count, forest: > =25%)	7.225	3.406	0	14.22	251982
Inverse hyperbolic sine transformation of Deforestation (pixel count, forest: > =50%)	6.636	3.688	0	14.216	251982
Price index	66.04	20.91	1.55	223.03	251982
Log Price index (ln Price)	4.14	0.32	0.436	5.41	251982
Distance to nearest seaport in km (dist. port)	596.35	431.63	1.81	1893.287	251982
Distance to capital city in km (dist. cap.)	911.47	817.44	1.77	7958.346	195986
Stable night-time lights in 2000 (night lights)	0.834	2.55	0	44.55	251982

Note: See SI Sections 9.1, 9.2 and 9.3 for more details.

9.5 Descriptive maps

Figure 5: Accumulated deforestation, 2001-2018

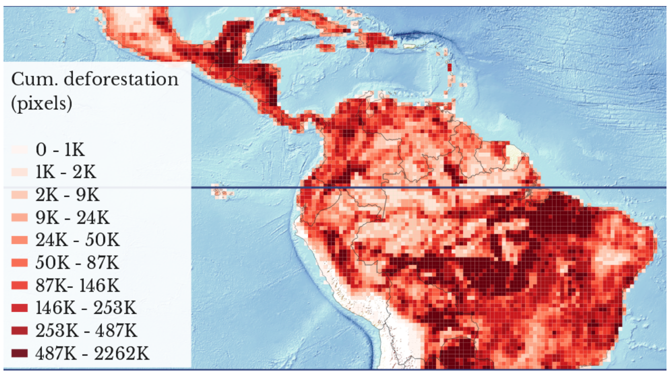

(a) Americas

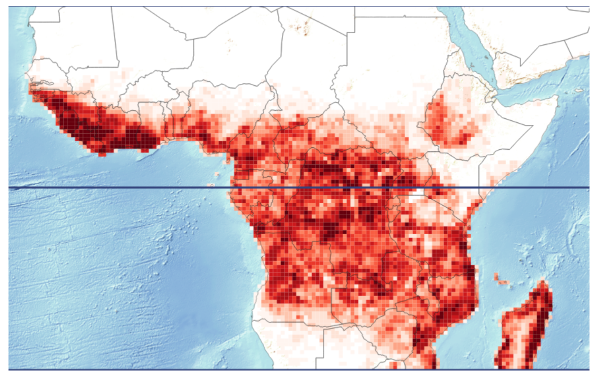

(b) Africa

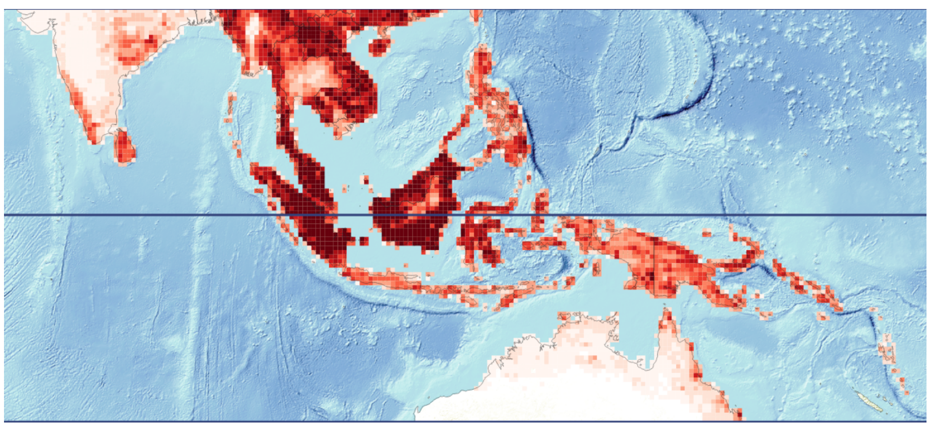

(c) Asia and Oceania

Note: Accumulated deforestation, in number of pixels (max. total of land pixel in a cell is 4000K), forest defined with a 25% threshold. Source: Hansen et al. (2013).

Figure 6: Average price index, 2001-2018

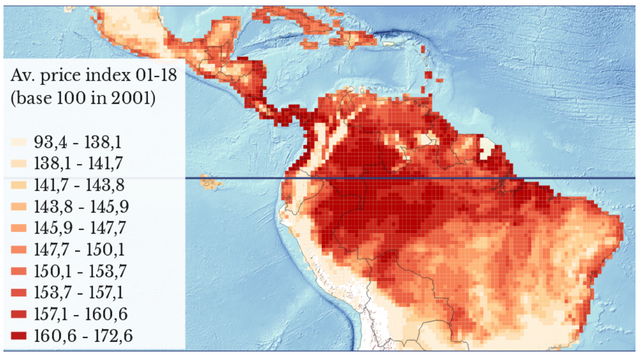

(a) Americas

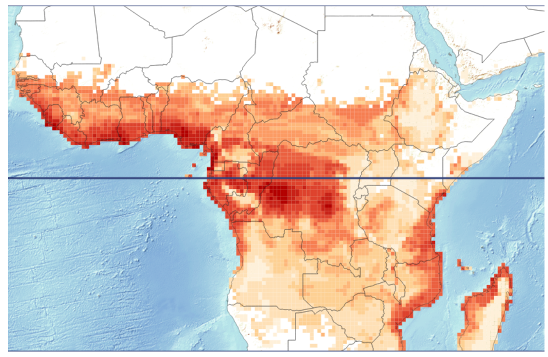

(b) Africa

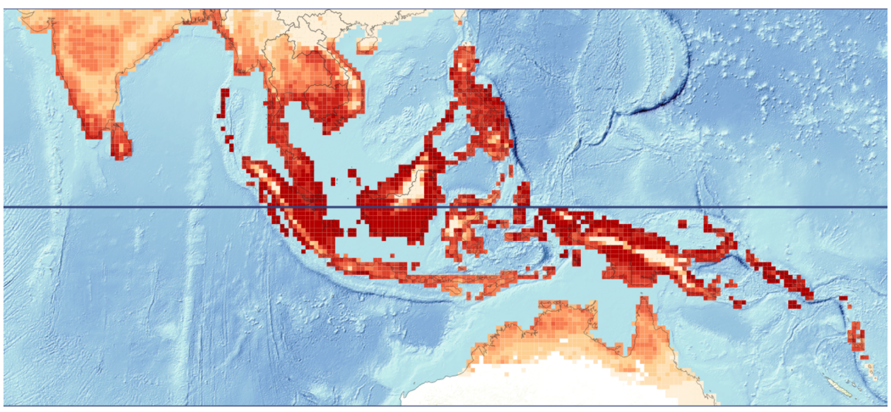

(c) Asia and Oceania

Note: Average value of the crop price index over the 2001-2018 period, taking 2001 as a base year.

Figure 7: Forest cover in 2000

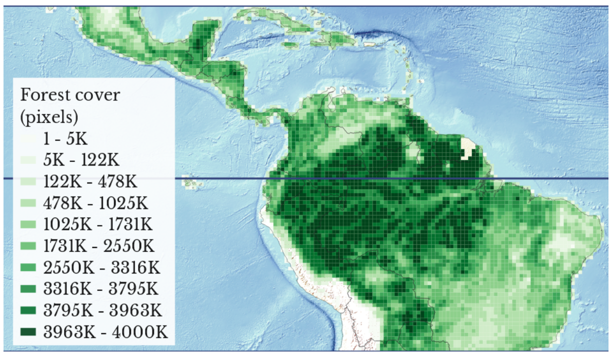

(a) Americas

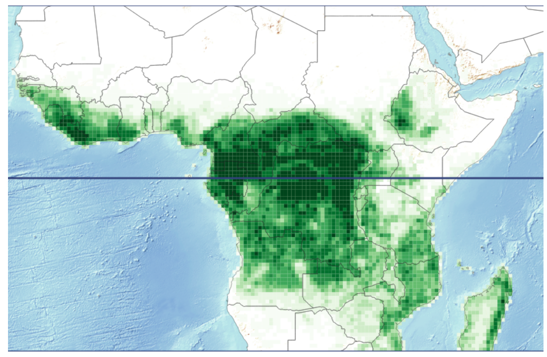

(b) Africa

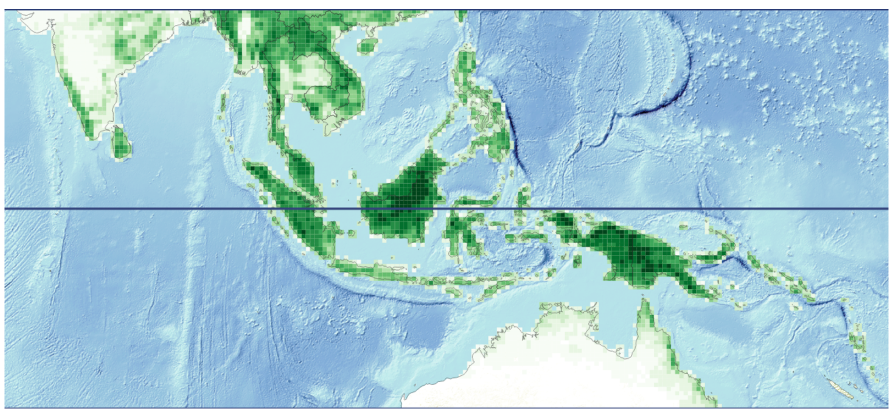

(c) Asia and Oceania

Note: Number of pixels covered by forest, using a 25% canopy cover threshold. Year: 2000. The maximum total of land pixels per cell is 4000K pixels.

10 Statistical analysis

10.1 Baseline estimates

This sub-section contains the two Tables related to the Figures displaying the baseline estimates in the manuscript. Table 2 displays the estimates used to construct Figure 1, Model 1 (Column 1) and Model 2 (Column 2). Table 3 shows the estimates used in Figure 3. Column (1) provides the estimates of Model 1, that is of specification (2) when we include interaction variables between the price index and cell characteristics (distance to the closest port, distance to the capital city and the intensity of nighttime lights). In column (2), we provide the estimates of the same specification, but with the price index interacted with a binary variable for each decile of the initial forest cover distribution. Finally, in column (3) we control for a full set of interactions between country dummies and the price index.

Table 2: Baseline results

	(1)	(2)
Model	Model 1	Model 2
ln Price	1.242^a	
	(0.081)	
× Cover[D1]		-0.199^b
		(0.099)
× Cover[D2]		0.185^c
		(0.100)
× Cover[D3]		0.826^a
		(0.096)
× Cover[D4]		1.002^a
		(0.094)
× Cover[D5]		1.164^a
		(0.093)
× Cover[D6]		1.218^a
		(0.090)
× Cover[D7]		1.497^a
		(0.092)
× Cover[D8]		1.623^a
		(0.089)
× Cover[D9]		1.929^a
		(0.086)
× Cover[D10]		2.265^a
		(0.089)
Cell FE	Yes	Yes
Country × Year FE	Yes	Yes
Observations	251982	251982
Countries	119	119
Period	2001-2018	2001-2018
R^2	0.910	0.911

Note: Least square estimator. ^{c} significant at 10%; ^{b} significant at 5%; ^{a} significant at 1%. Standard errors clustered at the cell level in parentheses. The dependent variable is the hyperbolic inverse sine of the number of pixels deforested in the cell. ln Price is our crop price index, defined in equation (2). Cover[x] are bins for deciles of forest cover in 2000.

Table 3: Baseline results with cell characteristics

	(1) Model 1	(2) Model 2	Model 3
ln Price	1.165^{a}		
	(0.080)		
× ln dist. port	-0.133^{a}	-0.306^{a}	-0.147^{a}
	(0.024)	(0.023)	(0.024)
× ln dist. cap.	0.172^{a}	0.029	0.153^{a}
	(0.024)	(0.024)	(0.025)
× night lights	-0.088^{a}	-0.059^{a}	-0.096^{a}
	(0.016)	(0.014)	(0.016)
× Cover[D1]		-0.242^{b}	
		(0.098)	
× Cover[D2]		0.120	
		(0.099)	
×Cover[D3]		0.759^{a}	
		(0.095)	
× Cover[D4]		0.938^{a}	
		(0.093)	
× Cover[D5]		1.113^{a}	
		(0.092)	
× Cover[D6]		1.173^{a}	
		(0.089)	
× Cover[D7]		1.446^{a}	
		(0.091)	
× Cover[D8]		1.639^{a}	
		(0.089)	
× Cover[D9]		2.004^{a}	
		(0.087)	
× Cover[D10]		2.380^{a}	
		(0.091)	
Cell FE	Yes	Yes	Yes
Country × Year FE	Yes	Yes	Yes
Country FE × price	No	No	Yes
Observations	251982	251982	251982
Countries	119	119	119
Period	2001-2018	2001-2018	2001-2018

Note: Least square estimator. [c] significant at 10%; [b] significant at 5%; [a] significant at 1%. Standard errors clustered at the cell level in parentheses. The dependent variable is the hyperbolic inverse sine of the number of pixels deforested in the cell. ln Price is our crop price index, defined in equation (2). Cover[x] are bins for deciles of forest cover in 2000. ln dist. port is the log of distance from the closest seaport. ln dist. cap. is the log of the distance from the country's capital city at the beginning of the period. night lights is the average amount of nighttime lights emitted in the cell in 2000.

10.2 Sensitivity analysis

Here we discuss a set of exercises to asses the sensitivity of our analysis. All exercises are implemented for Models 1 and 2. First, we consider an alternative canopy threshold that defines the tropical forest biome at 50% instead of 25%. Note that it reduces slightly the number of observation as few grid of 0.5 degree do not include any pixels of 30 meters with a 50% canopy cover in 2000 (Table 4, columns 1 and 2). Second, as our main dependent variable is a count of the number of deforested pixels, we estimate the models through a Poisson Pseudo-Maximum Likelihood (PPML) estimator instead of a Least Square Estimator (Table 4, columns 3 and 4). Third, we assess the sensitivity of the estimates of Models 1 and 2 to potential outliers (Table 5). Our main concern is that a small number of observations could drive our results. We exclude observations that are 3 (columns 1 and 4), 2 (columns 2 and 5) and 1 standard deviation (columns 3 and 6) away from the residual mean. Fifth, in the same vein, we want to ensure that our results are not driven by a small number of countries, especially those who might influence the world price of agricultural commodities (Table 6). Doing so, we exclude countries from the sample having the largest crop market shares: top 10% (columns 1 and 4), 25% (columns 2 and 5), and 50% (columns 3 and 6) largest crop market shares. The crops considered to compute the market shares are those included in our analysis: banana, barley, cocoa, coconut, coffee, cotton, maize, oil palm, rice, sorghum, soybean, sugar, tea, tobacco, wheat. Finally, the fine-grained dimension of our analysis makes it likely that the error term exhibits both spatial and serial correlation. To address this, we check that our results are robust to a non-parametric standard errors estimation [36, 55], allowing for both cross-sectional location-specific serial correlation, as well as spatial correlation within a 500 or 1000km radius (Table 7).

In section 10.2.2, from Table 8 to 11, we provide the same sensitivity analysis for the estimates including the cell-characteristics (Table 3, column 1 and 2).

10.2.1 Sensitivity: baseline specifications

Table 4: Sensitivity analysis of baseline estimates: canopy threshold & PPML

	(1)	(2)	(3)	(4)
Model	Model 1	Model 2	Model 1	Model 2
Canopy threshold	50%	50%	25%	25%
Estimator	OLS	OLS	PPML	PPML
ln Price	1.343^{a}		1.379^{a}	
	(0.082)		(0.117)	
× Cover[D1]		0.494^{a}		-1.925^{a}
		(0.099)		(0.278)
× Cover[D2]		0.299^{a}		0.476^{a}
		(0.100)		(0.157)
× Cover[D3]		0.614^{a}		0.929^{a}
		(0.099)		(0.142)
× Cover[D4]		0.881^{a}		0.967^{a}
		(0.097)		(0.131)
× Cover[D5]		1.022^{a}		1.164^{a}
		(0.097)		(0.133)
× Cover[D6]		1.152^{a}		1.067^{a}
		(0.093)		(0.127)
× Cover[D7]		1.503^{a}		1.234^{a}
		(0.093)		(0.125)
× Cover[D8]		1.686^{a}		1.413^{a}
		(0.091)		(0.126)
× Cover[D9]		2.024^{a}		1.768^{a}
		(0.087)		(0.124)
× Cover[D10]		2.347^{a}		1.899^{a}
		(0.090)		(0.147)
Cell FE	Yes	Yes	Yes	Yes
Country × Year FE	Yes	Yes	Yes	Yes
Observations	240732	240732	246559	246559

Note: Least square estimator in columns (1) and (2), PPML in columns (3) and (4). ^{c} significant at 10%; ^{b} significant at 5%; ^{a} significant at 1%. Standard errors clustered at the cell level in parentheses. The dependent variable is the hyperbolic inverse sine of the number of pixels deforested in the cell. ln Price is our crop price index, defined in equation (1). Cover[x] are bins for deciles of forest cover in 2000.

Table 5: Sensitivity analysis of the baseline estimates: dropping outliers

	(1)	(2)	(3)	(4)	(5)	(6)
Model	Model 1	Model 1	Model 1	Model 2	Model 2	Model 2
Sample: Excluded outliers	3 σ	2 σ	1 σ	3 σ	2 σ	1 σ
ln Price	1.100^a	0.974^a	0.899^a			
	(0.067)	(0.057)	(0.039)			
$\times$ Cover[D1]				-0.300^a	-0.298^a	-0.311^a
				(0.085)	(0.071)	(0.047)
$\times$ Cover[D2]				0.047	0.019	-0.086^c
				(0.083)	(0.069)	(0.047)
$\times$ Cover[D3]				0.675^a	0.586^a	0.478^a
				(0.079)	(0.067)	(0.045)
$\times$ Cover[D4]				0.834^a	0.720^a	0.608^a
				(0.078)	(0.066)	(0.045)
$\times$ Cover[D5]				0.973^a	0.851^a	0.697^a
				(0.078)	(0.067)	(0.046)
$\times$ Cover[D6]				1.035^a	0.941^a	0.810^a
				(0.077)	(0.067)	(0.045)
$\times$ Cover[D7]				1.287^a	1.168^a	1.051^a
				(0.078)	(0.067)	(0.046)
$\times$ Cover[D8]				1.429^a	1.320^a	1.184^a
				(0.076)	(0.066)	(0.045)
$\times$ Cover[D9]				1.739^a	1.603^a	1.465^a
				(0.073)	(0.063)	(0.043)
$\times$ Cover[D10]				2.106^a	1.961^a	1.761^a
				(0.076)	(0.066)	(0.045)
Cell FE	Yes	Yes	Yes	Yes	Yes	Yes
Country $\times$ Year FE	Yes	Yes	Yes	Yes	Yes	Yes
Observations	248299	239166	194598	248290	239175	194634

Note: Least square estimator. ^{c} significant at 10%; ^{b} significant at 5%; ^{a} significant at 1%. Standard errors clustered at the cell level in parentheses. The dependent variable is the hyperbolic inverse sine of the number of pixels deforested in the cell. ln Price is our crop price index, defined in equation (1). Cover[x] are bins for deciles of forest cover in 2000.

Table 6: Sensitivity analysis of the baseline estimates: dropping countries with a large crop market share

	(1)	(2)	(3)	(4)	(5)	(6)
Model	Model 1	Model 1	Model 1	Model 2	Model 2	Model 2
Sample: Excluded	Top 10%	Top 25%	Top 50%	Top 10%	Top 25%	Top 50%
ln Price	1.391^a	0.976^a	1.126^a			
	(0.088)	(0.101)	(0.132)			
× Cover[D1]				0.170	0.060	-0.228
				(0.109)	(0.116)	(0.168)
× Cover[D2]				0.382^a	0.247^b	0.419^b
				(0.109)	(0.118)	(0.169)
× Cover[D3]				0.901^a	0.768^a	0.835^a
				(0.105)	(0.116)	(0.161)
× Cover[D4]				1.010^a	1.065^a	1.113^a
				(0.103)	(0.118)	(0.160)
× Cover[D5]				1.148^a	1.157^a	1.352^a
				(0.103)	(0.119)	(0.167)
× Cover[D6]				1.213^a	1.209^a	1.307^a
				(0.099)	(0.112)	(0.156)
× Cover[D7]				1.491^a	1.510^a	1.566^a
				(0.102)	(0.117)	(0.163)
× Cover[D8]				1.624^a	1.648^a	1.715^a
				(0.099)	(0.117)	(0.159)
× Cover[D9]				1.985^a	1.793^a	1.894^a
				(0.094)	(0.111)	(0.150)
× Cover[D10]				2.420^a	1.983^a	2.078^a
				(0.098)	(0.125)	(0.163)
Cell FE	Yes	Yes	Yes	Yes	Yes	Yes
Country × Year FE	Yes	Yes	Yes	Yes	Yes	Yes
Observations	196506	146286	73782	196506	146286	73782

Note: Least square estimator. ^{c} significant at 10%; ^{b} significant at 5%; ^{a} significant at 1%. Standard errors clustered at the cell level in parentheses. The dependent variable is the hyperbolic inverse sine of the number of pixels deforested in the cell. ln Price is our crop price index, defined in equation (1). Cover[x] are bins for deciles of forest cover in 2000. In columns (1) and (4), we dropped the top 10% of the countries with respect to their average market share in our sample's crops post-2000 (top 25% in columns (2) and (5) and top 50% in columns (3) and (6)).

Table 7: Sensitivity analysis of the baseline estimates: Conley's standard errors

	(1)	(2)	(3)	(4)
Model	Model 1	Model 1	Model 2	Model 2
Spatial threshold	500km	500km	1000km	1000km
ln Price	1.242^a		1.242^a	
	(0.286)		(0.363)	
× Cover[D1]		-0.199		-0.199
		(0.288)		(0.352)
× Cover[D2]		0.185		0.185
		(0.285)		(0.342)
× Cover[D3]		0.826^a		0.826^a
		(0.271)		(0.320)
× Cover[D4]		1.002^a		1.002^a
		(0.270)		(0.316)
× Cover[D5]		1.164^a		1.164^a
		(0.271)		(0.318)
× Cover[D6]		1.218^a		1.218^a
		(0.273)		(0.323)
× Cover[D7]		1.497^a		1.497^a
		(0.279)		(0.330)
× Cover[D8]		1.623^a		1.623^a
		(0.282)		(0.334)
× Cover[D9]		1.929^a		1.929^a
		(0.282)		(0.345)
× Cover[D10]		2.265^a		2.265^a
		(0.295)		(0.356)
Observations	251982	251982	251982	251982
R^2	0.001	0.012	0.001	0.012
Cell FE	Yes	Yes	Yes	Yes
Country × Year FE	Yes	Yes	Yes	Yes
Observations	240732	240732	246559	246559

Note: Least square estimator. ^{c} significant at 10%; ^{b} significant at 5%; ^{a} significant at 1%. [36] standard errors allowing for infinite serial correlation and spatial correlation within a 500km or 1000km radius. The dependent variable is the hyperbolic inverse sine of the number of pixels deforested in the cell. ln Price is our crop price index, defined in equation (1). Cover[x] are bins for deciles of forest cover in 2000.

10.2.2 Sensitivity: specifications with cell characteristics

Table 8: Sensitivity analysis of specifications with cell characteristics: canopy threshold & PPML estimator

	(1)	(2)	(3)	(4)
Model	Model 1	Model 2	Model 1	Model 2
Canopy threshold	50%	50%	25%	25%
Estimator	OLS	OLS	PPML	PPML
ln Price	1.259^{a}		1.119^{a}	
	(0.081)		(0.111)	
× ln dist. port	-0.109^{a}	-0.318^{a}	-0.413^{a}	-0.481^{a}
	(0.026)	(0.025)	(0.035)	(0.035)
× ln dist. cap.	0.178^{a}	0.007	0.210^{a}	0.107^{a}
	(0.025)	(0.025)	(0.039)	(0.038)
× night lights	-0.096^{a}	-0.059^{a}	-0.091^{a}	-0.043^{b}
	(0.016)	(0.015)	(0.017)	(0.017)
× Cover[D1]		0.447^{a}		-2.114^{a}
		(0.098)		(0.273)
× Cover[D2]		0.238^{b}		0.197
		(0.099)		(0.154)
× Cover[D3]		0.552^{a}		0.579^{a}
		(0.097)		(0.137)
× Cover[D4]		0.819^{a}		0.606^{a}
		(0.096)		(0.124)
× Cover[D5]		0.973^{a}		0.860^{a}
		(0.096)		(0.127)
× Cover[D6]		1.111^{a}		0.783^{a}
		(0.092)		(0.122)
× Cover[D7]		1.460^{a}		0.927^{a}
		(0.092)		(0.120)
× Cover[D8]		1.716^{a}		1.165^{a}
		(0.091)		(0.120)
× Cover[D9]		2.120^{a}		1.578^{a}
		(0.088)		(0.120)
× Cover[D10]		2.491^{a}		1.791^{a}
		(0.093)		(0.141)
Cell FE	Yes	Yes	Yes	Yes
Country × Year FE	Yes	Yes	Yes	Yes
Observations	240732	240732	246559	246559

Note: Least square estimator in columns (1) and (2), PPML in columns (3) and (4). ^{c} significant at 10%; ^{b} significant at 5%; ^{a} significant at 1%. Standard errors clustered at the cell level in parentheses. The dependent variable is the hyperbolic inverse sine of the number of pixels deforested in the cell. ln Price is our crop price index, defined in equation (1). Cover[x] are bins for deciles of forest cover in 2000. ln dist. port is the log of distance from the closest seaport. ln dist. cap. is the log of the distance from the country's capital city at the beginning of the period. night lights is the average amount of nighttime lights emitted in the cell in 2000.

Table 9: Sensitivity analysis of specifications with cell characteristics: dropping outliers

	(1)	(2)	(3)	(4)	(5)	(6)
Model	Model 1	Model 1	Model 1	Model 2	Model 2	Model 2
Sample: Excluded outliers	3 σ	2 σ	1 σ	3 σ	2 σ	1 σ
ln Price	1.016^{a}	0.901^{a}	0.833^{a}			
	(0.067)	(0.057)	(0.039)			
$\times$ ln dist. port	-0.134^{a}	-0.128^{a}	-0.109^{a}	-0.300^{a}	-0.289^{a}	-0.265^{a}
	(0.021)	(0.018)	(0.012)	(0.020)	(0.018)	(0.012)
$\times$ ln dist. cap.	0.203^{a}	0.193^{a}	0.160^{a}	0.054^{a}	0.047^{a}	0.022^{c}
	(0.020)	(0.018)	(0.012)	(0.020)	(0.017)	(0.012)
$\times$ night lights	-0.097^{a}	-0.083^{a}	-0.070^{a}	-0.064^{a}	-0.051^{a}	-0.045^{a}
	(0.014)	(0.012)	(0.008)	(0.013)	(0.011)	(0.008)
$\times$ Cover[D1]				-0.340^{a}	-0.367^{a}	-0.359^{a}
				(0.084)	(0.071)	(0.047)
$\times$ Cover[D2]				-0.018	-0.062	-0.151^{a}
				(0.082)	(0.069)	(0.047)
$\times$ Cover[D3]				0.617^{a}	0.515^{a}	0.423^{a}
				(0.078)	(0.067)	(0.045)
$\times$ Cover[D4]				0.783^{a}	0.657^{a}	0.560^{a}
				(0.077)	(0.066)	(0.045)
$\times$ Cover[D5]				0.932^{a}	0.800^{a}	0.658^{a}
				(0.077)	(0.067)	(0.046)
$\times$ Cover[D6]				0.999^{a}	0.891^{a}	0.770^{a}
				(0.076)	(0.066)	(0.045)
$\times$ Cover[D7]				1.241^{a}	1.109^{a}	1.004^{a}
				(0.078)	(0.067)	(0.046)
$\times$ Cover[D8]				1.437^{a}	1.322^{a}	1.203^{a}
				(0.076)	(0.066)	(0.045)
$\times$ Cover[D9]				1.803^{a}	1.654^{a}	1.533^{a}
				(0.074)	(0.064)	(0.044)
$\times$ Cover[D10]				2.198^{a}	2.038^{a}	1.857^{a}
				(0.078)	(0.067)	(0.046)
Cell FE	Yes	Yes	Yes	Yes	Yes	Yes
Country $\times$ Year FE	Yes	Yes	Yes	Yes	Yes	Yes
Observations	248293	239160	194649	248280	239200	194709

Note: Least square estimator. ^{c} significant at 10%; ^{b} significant at 5%; ^{a} significant at 1%. Standard errors clustered at the cell level in parentheses. The dependent variable is the hyperbolic inverse sine of the number of pixels deforested in the cell. ln Price is our crop price index, defined in equation (1). Cover[x] are bins for deciles of forest cover in 2000. ln dist. port is the log of distance from the closest seaport. ln dist. cap. is the log of the distance from the country's capital city at the beginning of the period. night lights is the average amount of nighttime lights emitted in the cell in 2000.

Table 10: Sensitivity analysis of specifications with cell characteristics: dropping countries with a large crop market share

	(1)	(2)	(3)	(4)	(5)	(6)
Model	Model 1	Model 1	Model 1	Model 2	Model 2	Model 2
Sample: Excluded	Top 10%	Top 25%	Top 50%	Top 10%	Top 25%	Top 50%
ln Price	1.271[a]	0.959[a]	1.190[a]			
	(0.087)	(0.101)	(0.146)			
× ln dist. port	-0.067[b]	-0.045	-0.152[b]	-0.279[a]	-0.186[a]	-0.321[a]
	(0.027)	(0.043)	(0.063)	(0.026)	(0.041)	(0.061)
× ln dist. cap.	0.185[a]	-0.134[a]	0.201[c]	0.028	-0.128[a]	0.096
	(0.025)	(0.034)	(0.117)	(0.025)	(0.033)	(0.118)
× night lights	-0.115[a]	-0.141[a]	-0.104[a]	-0.077[a]	-0.104[a]	-0.059[c]
	(0.017)	(0.018)	(0.035)	(0.016)	(0.018)	(0.035)
× Cover[D1]				0.105	0.009	-0.285
				(0.109)	(0.117)	(0.177)
× Cover[D2]				0.306[a]	0.185	0.396[b]
				(0.108)	(0.118)	(0.181)
× Cover[D3]				0.834[a]	0.712[a]	0.846[a]
				(0.103)	(0.116)	(0.177)
× Cover[D4]				0.953[a]	1.017[a]	1.138[a]
				(0.102)	(0.118)	(0.174)
× Cover[D5]				1.102[a]	1.095[a]	1.357[a]
				(0.102)	(0.120)	(0.183)
× Cover[D6]				1.176[a]	1.151[a]	1.313[a]
				(0.097)	(0.113)	(0.169)
× Cover[D7]				1.447[a]	1.443[a]	1.556[a]
				(0.101)	(0.118)	(0.173)
× Cover[D8]				1.645[a]	1.590[a]	1.750[a]
				(0.098)	(0.117)	(0.167)
× Cover[D9]				2.052[a]	1.769[a]	1.950[a]
				(0.095)	(0.111)	(0.159)
× Cover[D10]				2.505[a]	1.980[a]	2.142[a]
				(0.101)	(0.125)	(0.170)
Cell FE	Yes	Yes	Yes	Yes	Yes	Yes
Country × Year FE	Yes	Yes	Yes	Yes	Yes	Yes
Observations	196506	146286	73782	196506	146286	73782

Note: Least square estimator. [c] significant at 10%; [b] significant at 5%; [a] significant at 1%. Standard errors clustered at the cell level in parentheses. The dependent variable is the hyperbolic inverse sine of the number of pixels deforested in the cell. ln Price is our crop price index, defined in equation (1). Cover[x] are bins for deciles of forest cover in 2000. In columns (1) and (4), we dropped the top 10% of the countries with respect to their average market share in our sample's crops post-2000 (top 25% in columns (2) and (5) and top 50% in columns (3) and (6)). ln dist. port is the log of distance from the closest seaport. ln dist. cap. is the log of the distance from the country's capital city at the beginning of the period. night lights is the average amount of nighttime lights emitted in the cell in 2000.

Table 11: Sensitivity analysis of specifications with cell characteristics: Conley standard errors

	(1)	(2)	(3)	(4)
	Model 1	Model 1	Model 2	Model 2
Spatial threshold	500	500	1000	1000
Estimator	OLS	OLS	OLS	OLS
ln Price	1.294^{a}		1.294^{a}	
	(0.293)		(0.362)	
× ln dist. port	-0.370^{b}	-0.760^{a}	-0.370^{c}	-0.760^{a}
	(0.183)	(0.173)	(0.201)	(0.184)
× ln dist. cap.	0.260	-0.040	0.260	-0.040
	(0.174)	(0.156)	(0.197)	(0.171)
× night lights	-0.037^{a}	-0.023^{b}	-0.037^{a}	-0.023^{b}
	(0.010)	(0.009)	(0.011)	(0.010)
× Cover[D1]		0.186		0.186
		(0.302)		(0.366)
× Cover[D2]		0.547^{c}		0.547
		(0.294)		(0.354)
× Cover[D3]		1.184^{a}		1.184^{a}
		(0.285)		(0.335)
× Cover[D4]		1.357^{a}		1.357^{a}
		(0.285)		(0.333)
× Cover[D5]		1.521^{a}		1.521^{a}
		(0.286)		(0.337)
× Cover[D6]		1.583^{a}		1.583^{a}
		(0.289)		(0.343)
× Cover[D7]		1.860^{a}		1.860^{a}
		(0.294)		(0.348)
× Cover[D8]		2.039^{a}		2.039^{a}
		(0.296)		(0.353)
× Cover[D9]		2.394^{a}		2.394^{a}
		(0.300)		(0.366)
× Cover[D10]		2.764^{a}		2.764^{a}
		(0.311)		(0.379)
Cell FE	Yes	Yes	Yes	Yes
Country × Year FE	Yes	Yes	Yes	Yes
Observations	251982	251982	251982	251982

Note: Least square estimator. ^{c} significant at 10%; ^{b} significant at 5%; ^{a} significant at 1%. [36] standard errors allowing for infinite serial correlation and spatial correlation within a 500km or 1000km radius. The dependent variable is the hyperbolic inverse sine of the number of pixels deforested in the cell. ln Price is our crop price index, defined in equation (1). Cover[x] are bins for deciles of forest cover in 2000. ln dist. port is the log of distance from the closest seaport. ln dist. cap. is the log of the distance from the country's capital city at the beginning of the period. night lights is the average amount of nighttime lights emitted in the cell in 2000.

10.3 Full quantification with cell-level characteristics

Figure 8 provides the same quantification as in Figure 4, but over all the Tropics.

Figure 8: Additional contrib. of cell-level characteristics, full Tropics sample

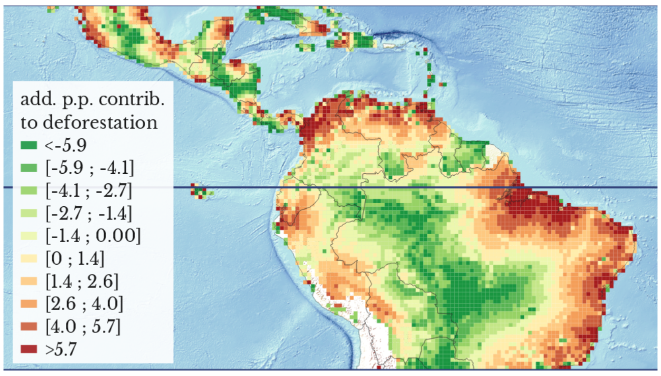

(a) Americas

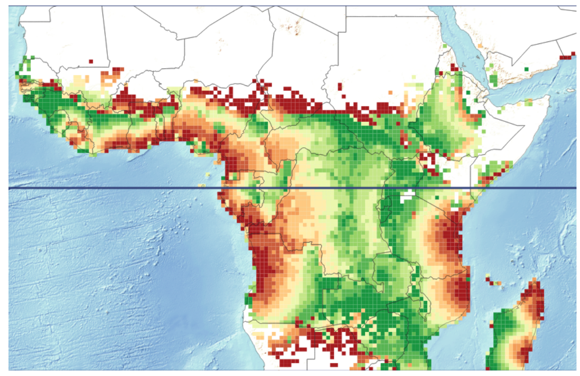

(b) Africa

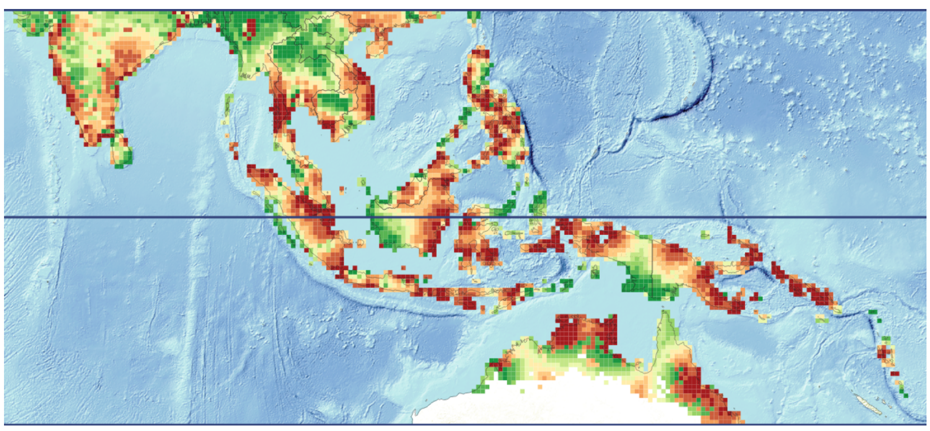

(c) Asia and Oceania

Note: This figure displays the difference (in percentage point) in the contribution of crop prices to deforestation when interacting variables with cell characteristics (Model 2, Figure 3), compared to our baseline (Figure 2). For each model, the quantification is computed in the following way. First, we compute the predicted level of deforestation using observed prices, our benchmark). Then, we compute a counterfactual level of deforestation assuming fixing prices at their 2001 level. Finally, we sum these predictions by cell over the period, and compute for each cell the contribution of prices as the difference between the benchmark and the counterfactual predictions, divided by the counterfactual.

CEE-M Working Papers[1] - 2021

WP 2021-01	Philippe Mahenc & **Alexandre Volle** « Price Signaling and Quality Monitoring in Markets for Credence Goods »
WP 2021-02	Mamadou Gueye, **Nicolas Quérou**, & **Raphael Soubeyran** « Inequality Aversion and the Distribution of Rewards in Organizations »
WP 2021-03	Lesly Cassin, Paolo Melindi-Ghidi & **Fabien Prieur** « Voting for environmental policy with green consumers: the impact of income inequality »
WP 2021-04	**Marion Davin** & **Emmanuelle Lavaine** « The Role Of Health At Birth And Parental Investment In Early Child Development. Evidence From The French ELFE Cohort »
WP 2021-05	**Koffi Serge William Yao**, **Emmanuelle Lavaine & Marc Willinger** « Does the approval mechanism induce the effcient extraction in Common Pool Resource games? »
WP 2021-06	**Raphaël Soubeyran** « Pro-social Motivations, Externalities and Incentives »
WP 2021-07	**Murielle Djiguemde, Dimitri Dubois, Alexandre Sauquet & Mabel Tidball** « Continuous versus Discrete Time in Dynamic Common Pool Resource Game Experiments »
WP 2021-08	**Marion Davin**, Mouez Fodha & Thomas Seegmuller « Environment, public debt and epidemics »
WP 2021-09	**Marc Willinger**, Oussama Rhouma & Klarizze Anne Puzon « Veto power and coalition formation in the commons: an experiment »
WP 2021-10	Yukihiko Funaki, **Emmanuel Sol**, **Marc Willinger** « Equal division among the few: an experiment about a coalition formation game »
WP 2021-11	**Koffi Serge William Yao**, **Emmanuelle Lavaine & Marc Willinger** « Effectiveness of the approval mechanism for CPR dilemmas: unanimity versus majority rule»

[1] **CEE-M Working Papers / Contact** : laurent.garnier@inrae.fr
- RePEc https://ideas.repec.org/s/hal/wpceem.html
- HAL https://halshs.archives-ouvertes.fr/CEE-M-WP/

WP 2021-12 **Sébastien Duchêne, Adrien Nguyen Huu, Dimitri Dubois & Marc Willinger**
« Why finance professionals hold green and brown assets? A lab-in-the-_eld experiment »

WP 2021-13 **Margaux Lapierre, Gwenolé Le Velly, Douadia Bougherara, Raphaële Préget, Alexandre Sauquet**
« Designing Agri-Environmental Schemes to cope with uncertainty »

WP 2021-14 Nicolas berman, Mathieu Couttenier, **Antoine Leblois** & **Raphael Soubeyran**
« Crop Prices and Deforestation in the Tropics»